INTERACTION OF OXYGEN WITH A LaB_6(310) SURFACE

Kevin Dale McKinstry
B.S., Colorado State University, 1983

A thesis submitted to the faculty
of the Oregon Graduate Center
in partial fulfillment of the
requirements for the degree
Master of Science
in
Applied Physics

September, 1985

The thesis "Interaction of Oxygen with a LaB_6(310) Surface" by Kevin D. McKinstry has been examined and approved by the following committee:

Paul R. Davis
Associate Professor
Thesis Research Advisor

Lynwood W. Swanson
Professor

Robert L. Martin
Professor
Lewis and Clark College

TABLE OF CONTENTS

LIST OF FIGURES

Figure 7 Thermal desorption of boron species from LaB_6(310) after an oxygen exposure of $7x10^{-5}$ torr-sec at 300 K. Curve a: B; curve b: BO; curve c: B_2O_2; curve d: B_2O_3. The vertical amplification factor for each curve is indicated and is relative to figs. 8, 10, 11, 12, 16, and 17.

Figure 8 Thermal desorption of lanthanum species from LaB_6(310) after an oxygen exposure of 10^{-4} torr-sec at 300 K. A boron oxide species from a slightly less oxygen exposure ($7x10^{-5}$ torr-sec) is shown for comparison. Curve a: La; curve b: LaO; curve c: BO. The vertical amplification factor for each curve is shown and is relative to other desorption spectra.

Figure 9 Variation with temperature of boron, oxygen, and lanthanum Auger peak-to-peak heights of LaB_6(310) after an oxygen exposure of $1.2x10^{-4}$ torr-sec at 930 K.

Figure 10 Thermal desorption of boron species from LaB_6(310) after an oxygen exposure of $7x10^{-5}$ torr-sec at 1270 K. Curve a: B; curve b: BO; curve c: B_2O_2; curve d: B_2O_3. The vertical amplification factor for each curve is shown and is relative to other desorption spectra.

Figure 11 Thermal desorption of lanthanum species from LaB_6(310) after an oxygen exposure of 10^{-4} torr-sec at 1440 K. A boron oxide species from a lesser oxygen exposure ($7*10^{-5}$ torr-sec) and lower temperature (1270 K) is shown for comparison. Curve a: La; curve b: LaO; curve c: BO. The vertical amplification factor for each curve is shown and is relative to other desorption spectra.

Figure 12 Thermal desorption of oxide species from LaB_6(310) after an oxygen exposure of $1.2x10^{-3}$ torr-sec at 1600 K. Curve a: BO; curve b: B_2O_2; curve c: B_2O_3; curve d: LaO. The vertical amplification factor for each curve is shown and is relative to other desorption spectra.

Figure 13 Variation with increasing temperature of boron, oxygen,and lanthanum Auger peak-to-peak heights of LaB_6(310) after an oxygen exposure of $2x10^{-3}$ torr-sec at 1600 K.

Figure 14 Variation with increasing temperature of boron, oxygen, and lanthanum Auger peak-to-peak heights of LaB_6(310) in an oxygen pressure of $2x10^{-7}$ torr.

LIST OF TABLES

ABSTRACT

Interaction of Oxygen with a

LaB_6(310) Surface

Kevin Dale McKinstry, M.S.

Oregon Graduate Center, 1985

Supervising Professor: Paul R. Davis

The interaction of oxygen with the (310) surface of LaB_6 has been investigated using Auger electron spectroscopy and mass spectrometric analysis. Measurements were made on both preadsorbed layers of oxygen and in fixed oxygen pressures. Desorption products observed were BO, B_2O_2, B_2O_3, and LaO. Oxygen saturation of the surface at room temperature was observed with adsorptions of 50L. Oxides on the surface appear as B_2O_3 and an unidentified lanthanum bearing oxide. Temperature and pressure dependencies of the desorption products were studied in detail. Facetting of the surface into (100) planes was observed.

I. INTRODUCTION

Lanthanum hexaboride (LaB_6) has received much attentionas a prime material for the construction of high brightness thermionic electron sources. First described by Lafferty [1], it is a refractory compound of good conductivity, low work function and low volatility at normal operating temperatures. Its implementation in successful cathode structures, however, requires that it be properly characterized in terms of surface properties and reactivity to residual gases in its operating environment.

The crystallographic dependence of the work function of LaB_6 has been well documented [2-6]. Depending on which crystal plane is exposed at the surface, work functions as low as 2.4 eV have been found, and generally these low work function planes have been shown to be thermally stable (with respect to macroscopic properties) as well. In particular, Gesley and Swanson [6] have shown the (310) surface of LaB_6 to be thermally stable and to possess the lowest work function yet found in this material (2.4 eV), making it a good candidate for thermionic emitters.

Residual gases in a thermionic emitter's operating environment can influence its operation by interacting with the cathode surface, significantly changing its properties by the formation of foreign surface layers. These layers in turn can affect both the work function and the structure of the emitting surface. Contaminant gases such as oxygen, water, or methane can form volatile compounds on the surface

causing evaporation of material and hence considerably shorten its lifetime. Since oxygen is one of the more reactive and abundant gases, how it reacts with the cathode is an important consideration.

The effects of oxygen on different LaB_6 crystal planes have been studied in some detail, in particular on the (100) surface [7-14]. Findings include marked work function increases after oxygen adsorption, incongruent vaporization of La and B, and formation and evaporation of boron and lanthanum oxides when oxygen is adsorbed on the heated surface. Other findings noted were preferential evaporation of the surface in the <100> direction and room temperature adsorption of oxygen saturating at 15-16 L (1L = 10^{-6} Torr-sec).

Similar studies have been done on the (110), (111), and (210) faces of LaB_6 [10,15,16]. The (110) and (111) surfaces also showed preferential evaporation in the <100> direction. In all cases room temperature adsorption of oxygen was found to saturate at 15-16L.

The focus of this work is similar to the above studies but concerns the interaction of oxygen with the (310) surface of LaB_6. Measurements are done on both the clean and oxidized surfaces using Auger electron spectroscopy (AES) for surface analysis and mass spectrometry for analysis of the desorbing molecular species. These experimental techniques allow the acquisition of information on the nature of surface oxide species and their thermal evaporation characteristics and, if used in conjunction with fixed pressures of oxygen, on the formation and removal of various oxide species under conditions similar to actual cathode operation.

II. EXPERIMENT

The sample used in the experiments consisted of a single crystal LaB_6 (precise stoichiometry $LaB_{6.09}$) disk 4 mm in diameter, aligned in the <310> direction and highly polished on the exposed face. The LaB_6 disk was mounted in a rhenium cup by FEI Co., using a proprietary braze. The assembly was resistively heated by passing current through rhenium wires spot welded to the back. The sample was prepared and analyzed as previously described [17].

All measurements were done with the sample mounted on a Huntington model 600 manipulator stage, enabling it to face either the mass spectrometer or Auger optics as shown in Figure 1. The mass spectrometer used was an EAI series 200 Quadrupole Residual Gas Analyzer and the Auger spectrometer was a PerkinElmer Physical Electronics model 10-155 Auger electron spectrometer with a cylindrical mirror analyzer operating in the derivative mode. Output from the mass spectrometer electron multiplier was routed to a Keithley model 600 electrometer, used as a low noise, high gain signal amplifier. Oxygen was released into the vacuum system through a Varian leak valve and monitored by a nude Bayard-Alpert ionization gauge; the vacuum system itself was pumped by a Perkin-Elmer 200 l/s ion pump assisted by titanium sublimation pumps. Base pressure of the entire system was 2×10^{-10} torr.

In order to monitor sample temperatures during heating cycles a W5%Re/W26%Re thermocouple was spot welded to the side of the rhenium cup. Because the thermocouple could not be attached directly to the

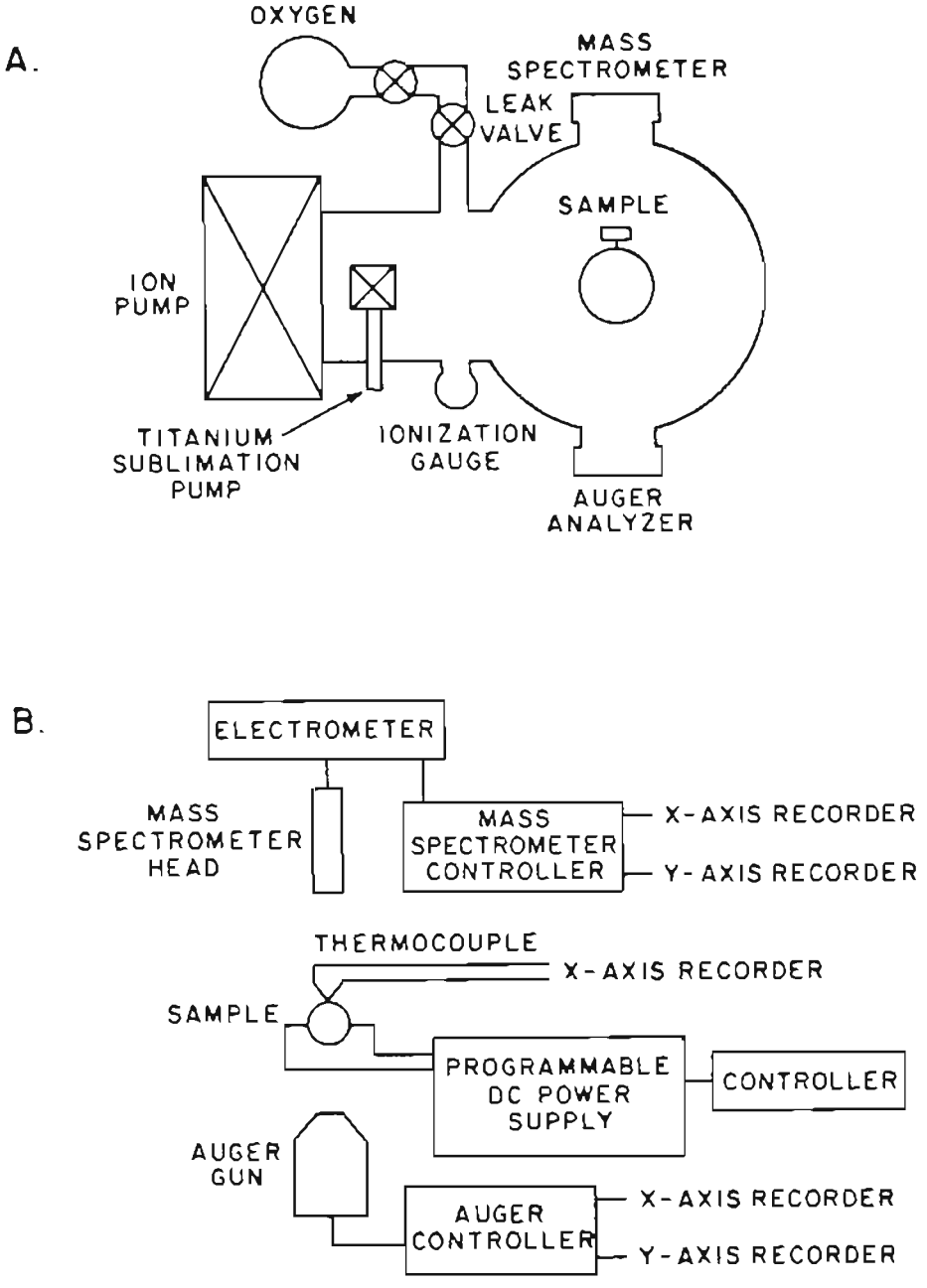

Figure 1 Diagram of the experimental apparatus. Part A: the physical apparatus; part B: the electronics used in conjunction with the physical apparatus.

sample, its ouput was calibrated against sample temperature using an optical pyrometer, correcting for the pyrex observation window and using the emissivity found by Storms [18] for LaB_6. Possible diffusion of rhenium between the thermocouple wires and sample cup was first considered to be a potential problem but periodic recalibration of the thermocouple showed this concern to be unfounded. A plot of sample temperature in K versus thermocouple output in mV is shown in Figure 2.

Sample heating current was supplied by a Sorenson model 40-12 programmable power supply operated in the regulated current mode. The output current was ramped linearly, producing sample temperature profiles as shown in Figure 3. All experiments involving preadsorbed layers of oxygen were performed using the fast temperature sweep. A slower sweep was used while the sample was exposed to constant pressures of oxygen in order to better simulate steady state conditions.

Desorption experiments were carried out by first flashing the sample at 1700 K to clean the surface. After cleaning, the sample was allowed to cool to the temperature at which oxygen was to be adsorbed. That temperature was then held by continuing to pass current through the heating filaments on the back of the rhenium cup. Next, oxygen was leaked into the system to a known pressure as measured by the ionization gauge. This pressure was maintained within the system for the time necessary to allow adsorption of the amount of oxygen dictated by the particular experiment, after which the leak valve was closed. The sample was then cooled as necessary to room temperature and the vacuum system allowed to pump down to background pressure. After rotating the sample to its position in front of the mass spectrometer ionizer head,

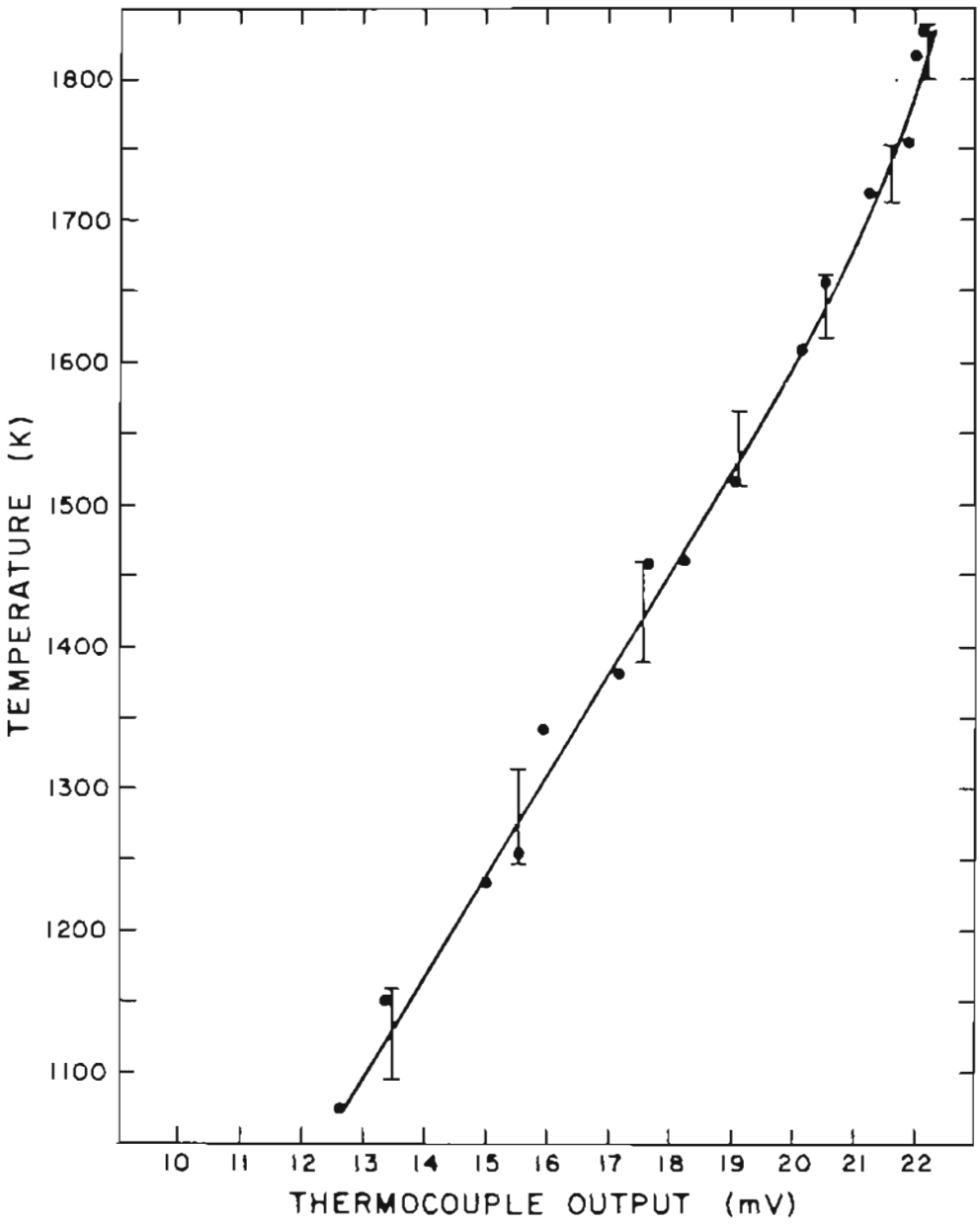

Figure 2 A plot of sample temperature vs. thermocouple output used in the experiment.

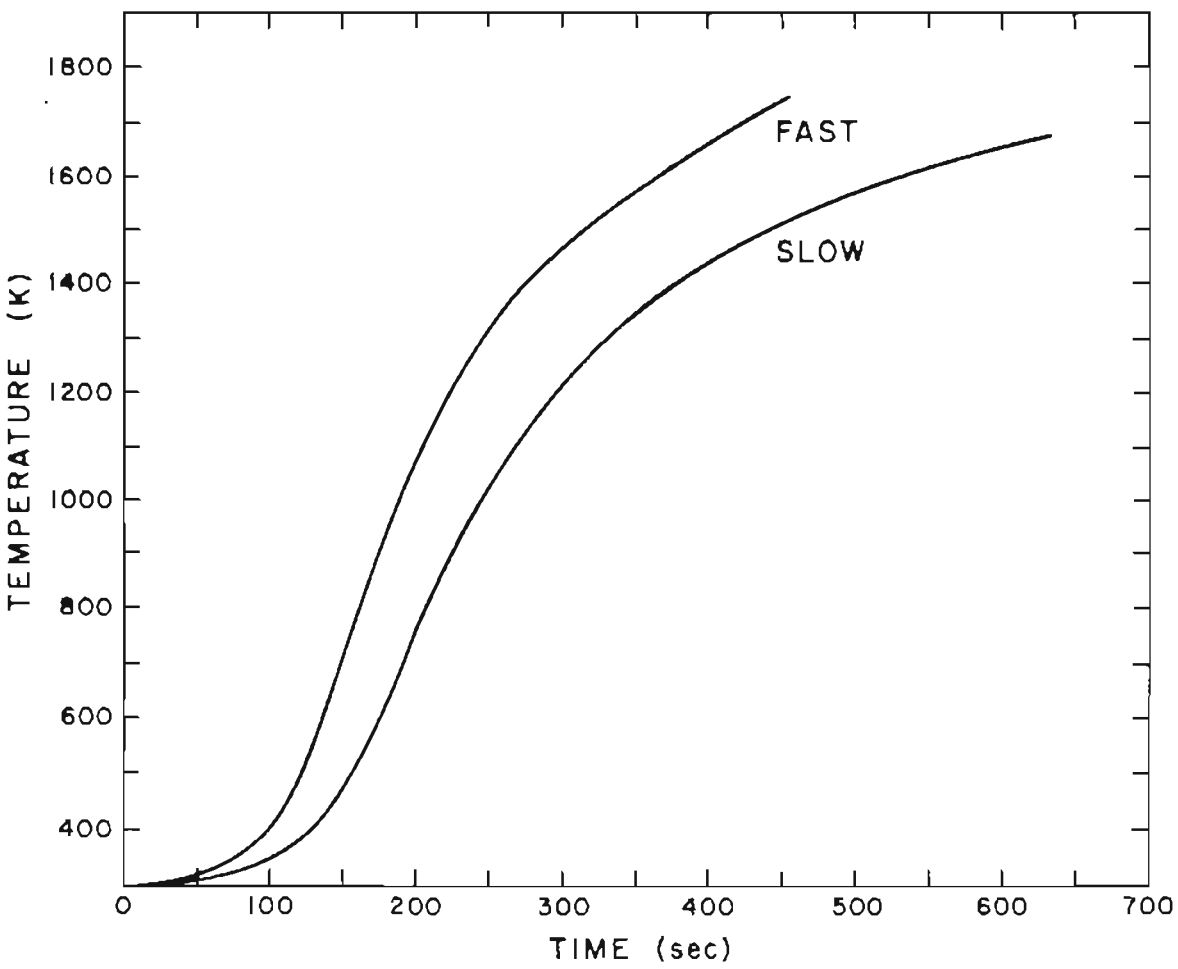

Figure 3 A plot of sample temperature vs. time for the two temperature ramp speeds used.

the heating current was slowly increased while outputs from both the electrometer and thermocouple were monitored.

Auger spectroscopic desorption analysis proceeded in a similar fashion. The sample was flashed clean, oxygen was adsorbed , and the sample was turned to its position in front of the Auger optics. Each atomic species was monitored by repetitively scanning the Auger analyzer over a pass energy window just sufficient to record the main spectrum peak of that element. Then as sample temperature was increased a plot of Auger peak height vs. thermocouple output was recorded. Since the electron beam from the Auger analyzer itself can cause surface changes by electron stimulated desorption [19], observations were made on the Auger oxygen peak (503 eV) in order to gauge the severity of this process. It was found that electron beam desorption for the experimental conditions used had minimal effects when compared to temperature induced desorption.

All studies of heating in oxygen were performed in virtually the same manner as the flash desorption experiments. Instead of adsorbing oxygen after the sample was flashed clean, however, oxygen was leaked into the system at a constant pressure which was maintained for the remainder of the experiment. Sufficient time was allowed before heating the sample to assure equilibrium between the sample surface and gas in the system. At the end of each run the leak valve was closed, reducing the oxygen pressure to its background value, and the sample was flashed clean.

III. EXPERIMENTAL RESULTS

The surface concentrations of oxygen on LaB_6 were first investigated using Auger spectroscopy. Figure 4 shows the relative oxygen peak-to-peak height as a function of oxygen dose while the sample remained at room temperature. With oxygen exposures up to 10L the oxygen coverage on the surface increases rapidly, while at greater exposure the increase is more gradual, with the surface saturating at approximately 50L. At higher doses the oxygen signal from the surface increases even more slowly but linearly, probably forming a thicker oxide coating. Oxygen coverage was a function of exposure and independent of pressure for pressures below 10^{-6} torr.

Figure 5 compares Auger spectra for three different surface conditions: clean, with saturated oxygen coverage (100L oxygen exposure at room temperature), and with a thicker oxide coating formed at a high temperature (1000L oxygen exposure at 1600 K). The clean surface shows a boron to lanthanum ratio (corrected for relative Auger transition sensitivities) of about four to one and with monolayer oxygen coverage about two to one, based on derivative peak-to-peak heights. Substantial curve shape changes can also be seen in both the boron and lanthanum spectra, indicating some sort of bonding of oxygen to both atomic species. Even more drastic peak shape changes are seen with the fully oxidized surface which might be an indication of more or stronger bonding between the elements in the surface layer probed by AES. There was no observed shift in the La(MNN) peak under any

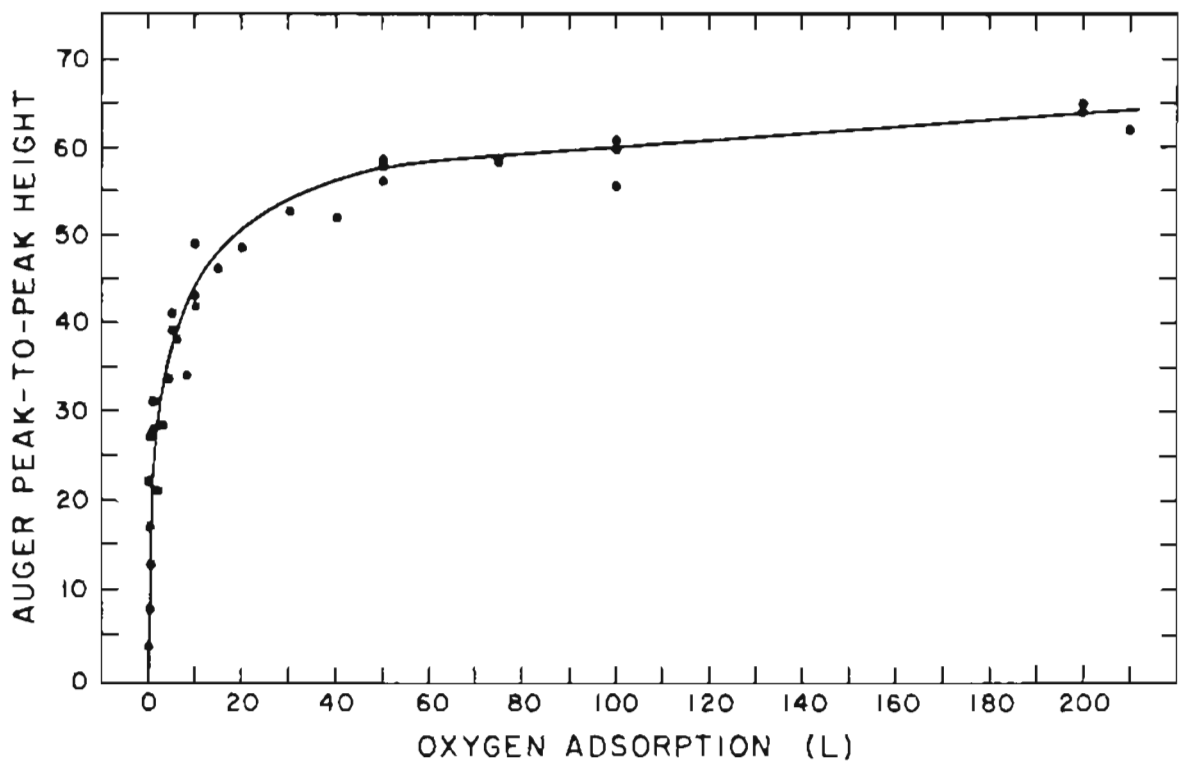

Figure 4 A plot of Auger peak-to-peak height vs. oxygen adsorption on LaB_6(310) at room temperature. Adsorption at room temperature was indepenent of pressure.

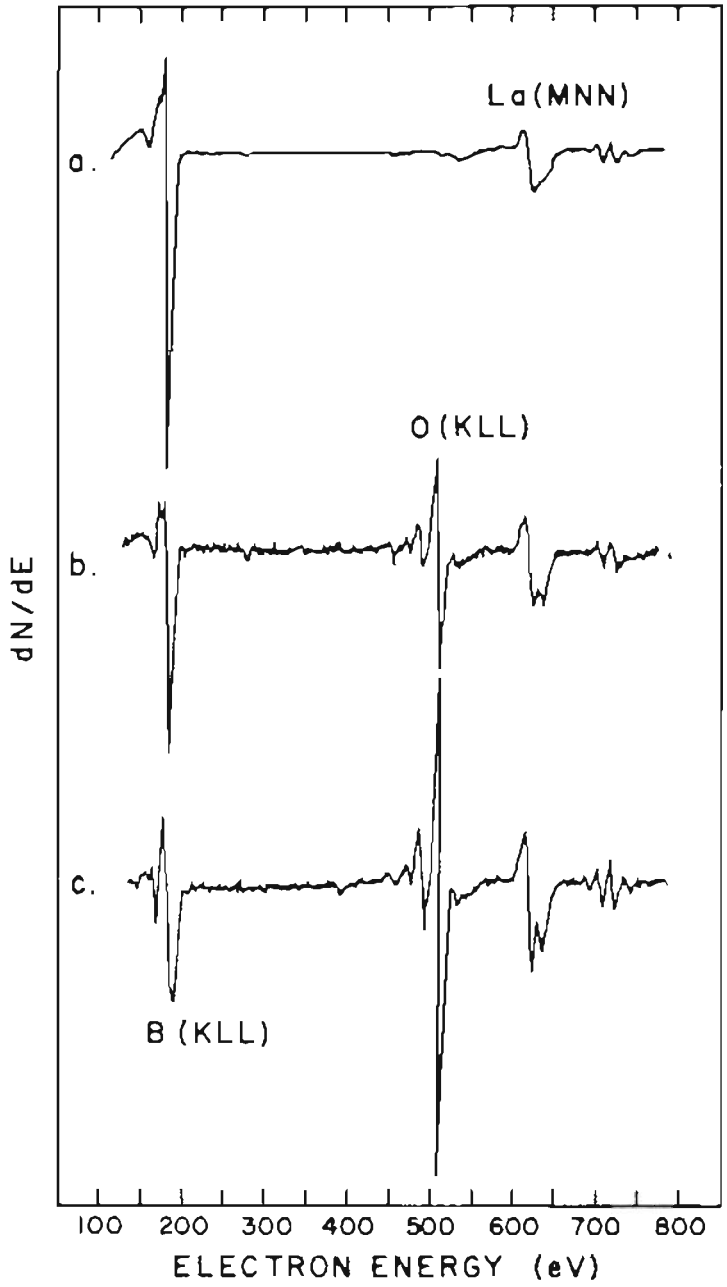

Figure 5 Auger spectra of LaB_6(310) for three different oxidation conditions. Curve a: clean surface; curve b: room temperature oxygen saturation (10^{-4} torr-sec); curve c: fully oxidized surface (1.2×10^{-3} torr-sec at 1600 K).

oxidation conditions used.

Mass spectrometric analysis of desorption from oxygen covered LaB_6(310) produced evidence of many desorbing molecular species. The observed species and their detection conditions are summarized in Table 1, along with those species monitored but not detected under any of the experimental procedures used. The detection of any O (mass 16) or O_2 (mass 32) desorbing from the surface was prevented by oxygen ambient in the system and oxygen desorption from the sample support structure.

Surface conditions monitored during desorption of oxygen from the surface using AES are plotted as relative peak-to-peak signal height of each element vs. temperature. Figure 6 shows this type of information for thermal desorption of monolayer coverage of oxygen (100L) from the surface. All of the observed signals remain fairly constant until 1250 K where the boron signal is at its minimum and the oxygen signal is at maximum. At this temperature the boron signal increases rapidly until 1300 K at which point it again stabilizes. Increasing again at 1450 K, it peaks at 1600 K and begins a gentle decline. The oxygen signal shows a sharp decline at 1400 K, followed by a slow fall up to 1650 K where the surface shows no oxygen coverage. In contrast to the boron and oxygen signals the lanthanum signal is almost constant throughout the entire temperature range, showing only a small broad peak at 1500 K.

Figure 7 shows desorption product curves produced from a similar oxygen exposure (70L); the species curves shown in this figure are B, BO, B_2O_2, and B_2O_3 and have been corrected as previously described [13] for varying mass sensitivity of the mass spectrometer. Each curve is

Mass	Species	Detection Conditions	Comments
11	B^+	T~1800 K clean or with adsorbed O	lower temperature peaks observed from fragmentation of boron oxides
27	BO^+	observed after any oxygen exposure	lower temperature peak observed after exposure of 1L; dominant B oxide desorbed
43	BO_2^+	not observed	
54	$B_2O_2^+$	observed after any oxygen exposure	
69.5	La^{++}	same as La^+	
70	$B_2O_3^+$	seen after oxygen exposure of >10L	
139	La^+	T~1700 K clean or with adsorbed O	shows fragmentation peak from LaO with adsorbed oxygen
155	LaO^+	observed after any oxygen exposure	
326	$La_2O_3^+$	not observed	

Table 1 Thermal desorption of oxides from LaB_6(310): Species monitored

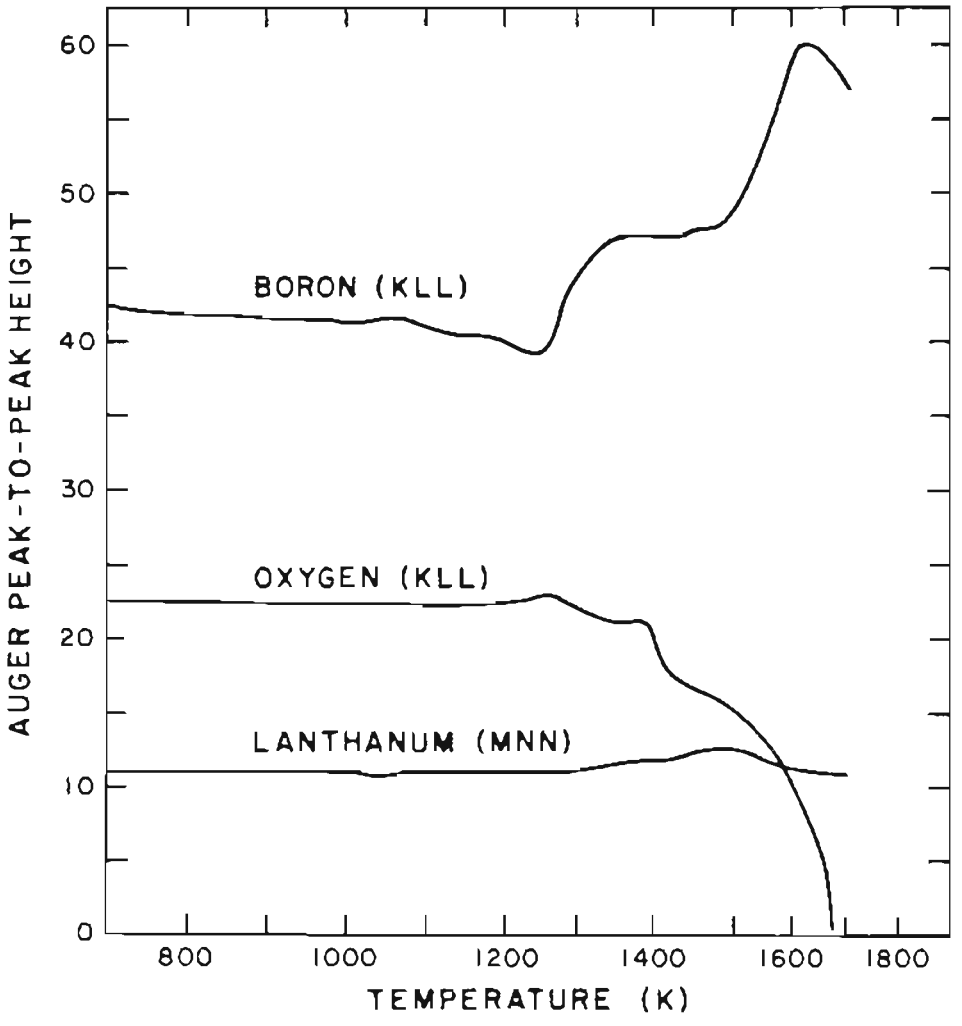

Figure 6 Variation with temperature of boron, oxygen, and lanthanum Auger peak-to-peak heights of LaB_6(310) after an oxygen exposure of 1.2×10^{-4} torr-sec at 300 K.

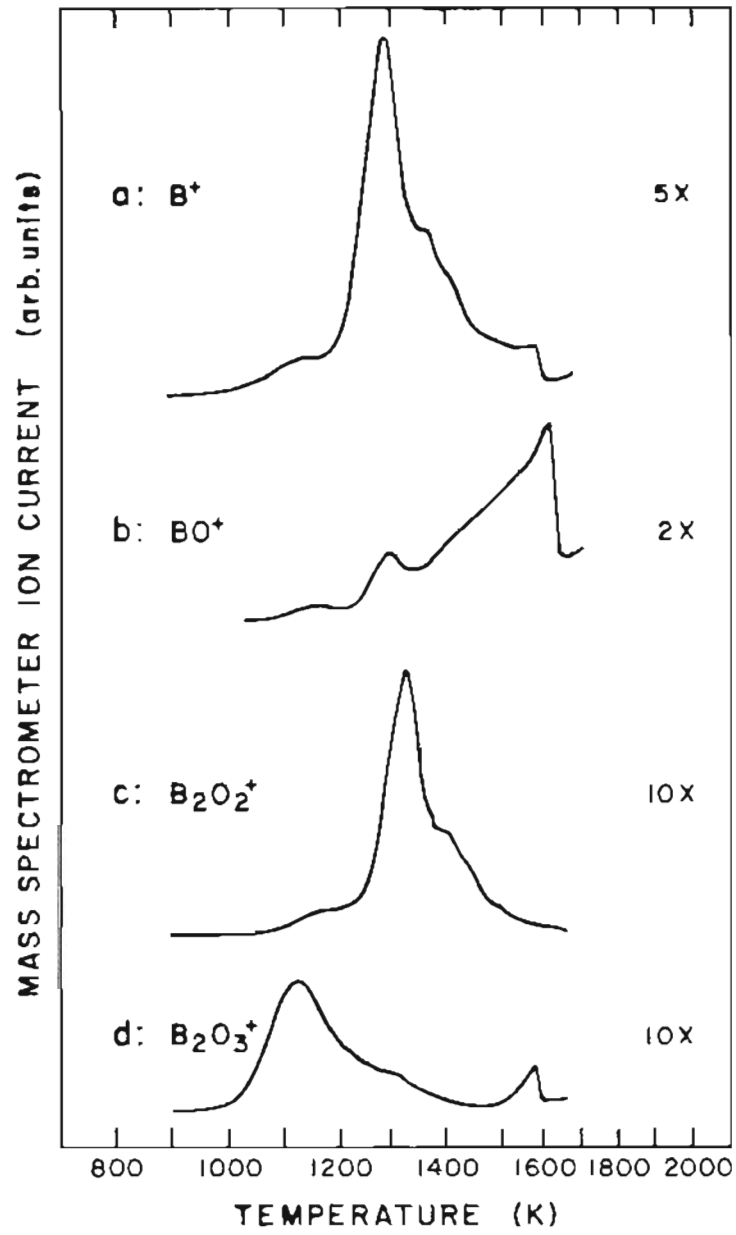

Figure 7 Thermal desorption of boron species from LaB_6(310) after an oxygen exposure of $7x10^{-5}$ torr-sec at 300 K. Curve a: B; curve b: BO; curve c: B_2O_2; curve d: B_2O_3. The vertical amplification factor for each curve is indicated and is relative to Figures 8, 10, 11, 12, 16, and 17.

labeled as to its relative sensitivity. All boron containing species in this case are first observed at 1000 K but reach their maxima at different temperatures. The oxide B_2O_3 reaches its maximum desorption rate at 1140 K with a secondary shoulder at 1300 K, where B, BO, and B_2O_2 have desorption rate maxima. The peak seen at 1600 K in the B_2O_3 (average mass/charge = 69.6) curve can be attributed to doubly ionized La (average mass/charge = 69.5), as the mass spectrometer resolution is insufficient to separate these two species. Similar desorption curve shapes of B and B_2O_2 between 1200 K and 1500 K suggest that some, if not all, B in this case comes from the breakdown of B_2O_2 within the mass spectrometer ionizer. The shoulder features at 1650 K of the B and BO curves are probably related in the same fashion. Since all oxygen is gone from the surface by 1650 K, it is clear that BO is the dominant boron containing desorption product.

Lanthanum bearing desorption product curves, as shown in Figure 8, have been produced after an oxygen exposure of 100L. As a comparison the BO desorption spectrum of Figure 7 has been included. As indicated in the figure there is no apparent desorption of either La or LaO from the surface until 1500 K, at which point the desorption rates for both species increase rapidly with temperature. This increase ends only after all oxygen has been removed from the surface. Similarities between the La and LaO desorption curves again suggest that La is a fragmentation product of LaO. The high temperature tails seen on most curves illustrated in this and the preceding figure are clearly from a source other than the sample surface as no oxygen remains on the surface at temperatures above 1650 K.

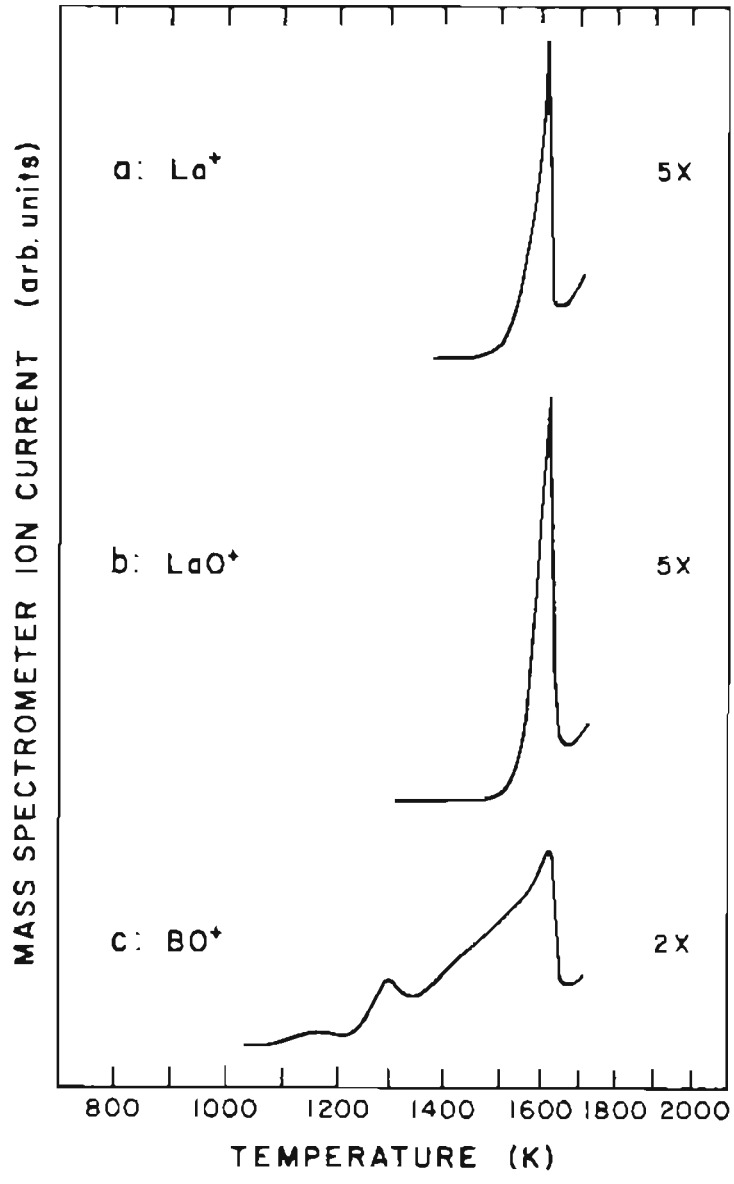

Figure 8 Thermal desorption of lanthanum species from LaB_6(310) after an oxygen exposure of 10^{-4} torr-sec at 300 K. A boron oxide species from a slightly less oxygen exposure ($7x10^{-5}$ torr-sec) is shown for comparison. Curve a: La; curve b: LaO; curve c: BO. The vertical amplification factor for each curve is shown and is relative to other desorption spectra.

If the same amount of oxygen is adsorbed at temperatures around 1000 K, as shown in the AES surface profiles of Figure 9, more oxygen remains on the surface and the spectrum features first seen in Figure 6 become more distinct. The boron signal curve consists of two peaks at 1350 K and 1600 K superposed on a rise beginning at 1100 K and ending at 1650 K. Maxima in the boron signal curve are echoed by minima in the oxygen signal curve, resulting in the "terraced" structure shown. The lanthanum signal curve is again fairly constant, with only a broad peak centered at 1400 K observed. As in Figure 6 all oxygen has been removed from the surface at 1650 K.

Desorption product curves from a similarly oxidized surface are shown in Figures 10 and 11. All of the desorption products observed, with the exception of La and LaO, begin to desorb from the surface at temperatures around 1200 K in contrast to the 1000 K temperature for room temperature adsorption. The B desorption curve still shares several common peaks with the other boron containing species but now has a significant peak at 1350 K which is not shared by any other species. The main peak in the B_2O_3 desorption spectrum has shifted 200 K upward and contains no sub-peaks in contrast to the other boron oxide desorption spectra which have developed several sharply defined sub-peaks. There are no apparent changes in the La and LaO spectra shapes, although the greater amount of oxygen adsorbed on the surface has increased their amplitudes and shifted their declines upward 50 K.

For the surface which has been oxidized at high temperature (1000 L at 1600 K) desorption temperatures of all the observed species have risen dramatically, as shown in Figure 12. Desorption of B_2O_3 begins

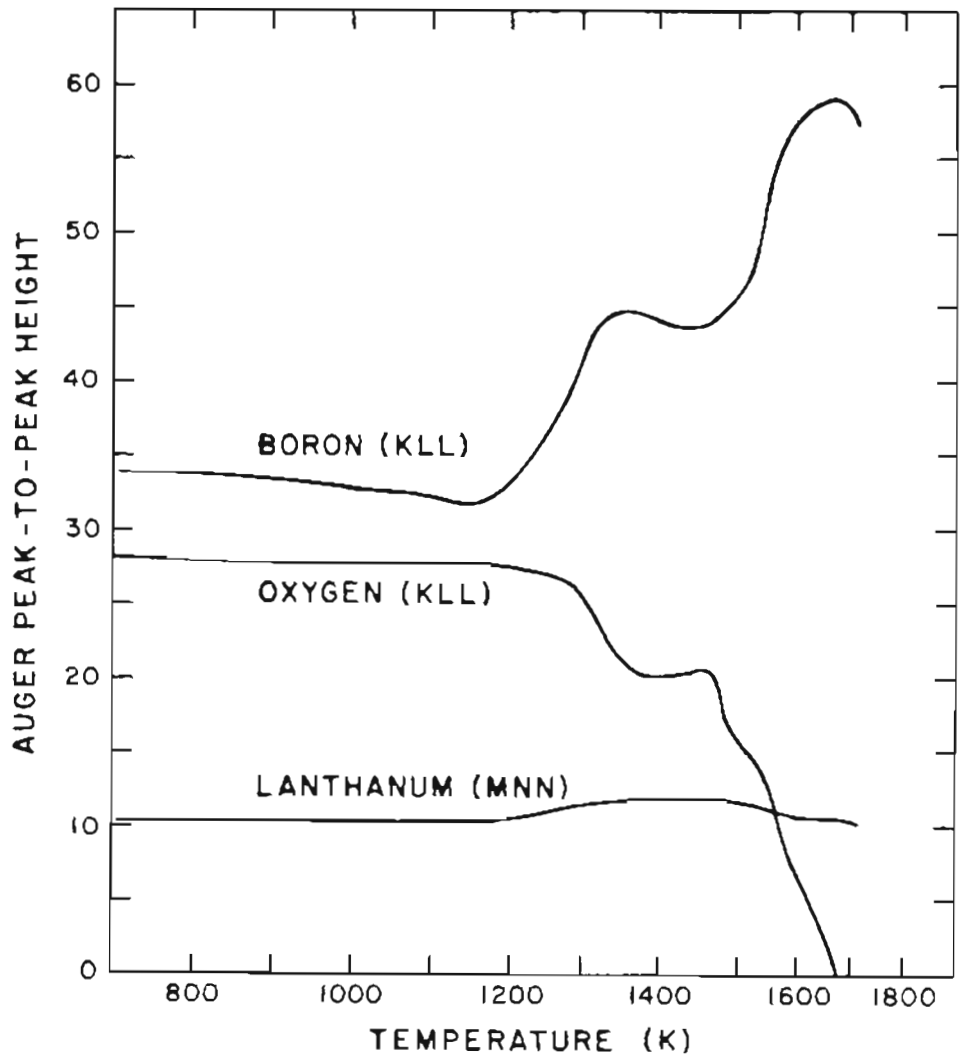

Figure 9 Variation with temperature of boron, oxygen, and lanthanum Auger peak-to-peak heights of LaB_6(310) after an oxygen exposure of 1.2×10^{-4} torr-sec at 930 K.

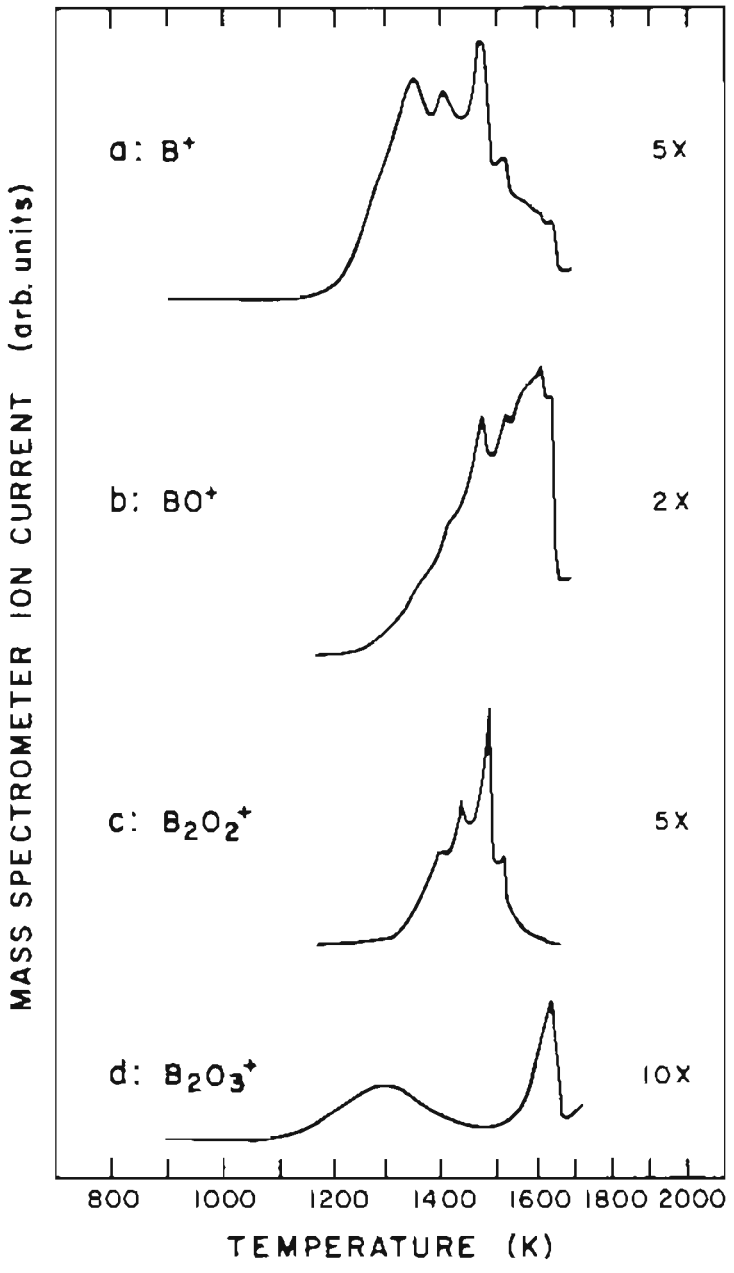

Figure 10 Thermal desorption of boron species from LaB_6(310) after an oxygen exposure of 7×10^{-5} torr-sec at 1270 K. Curve a: B; curve b: BO; curve c: B_2O_2; curve d: B_2O_3. The vertical amplification factor for each curve is shown and is relative to other desorption spectra.

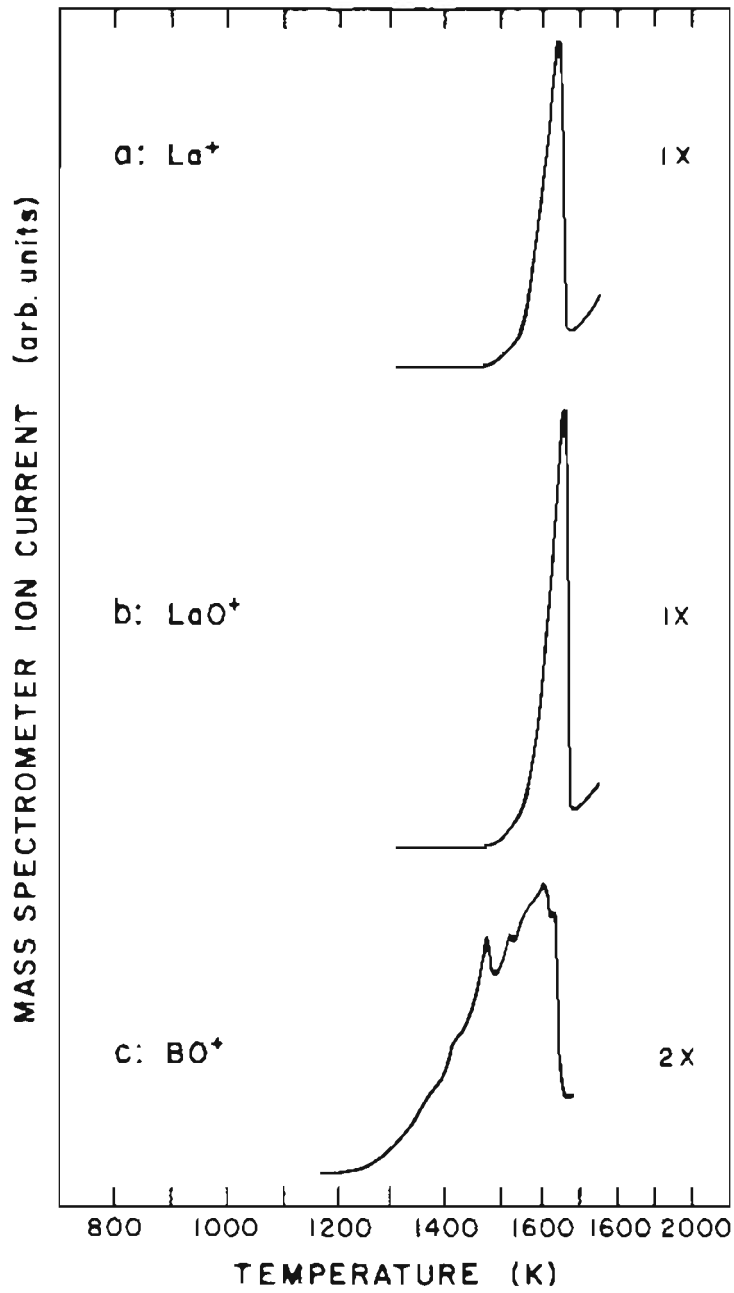

Figure 11 Thermal desorption of lanthanum species from LaB_6(310) after an oxygen exposure of 10^{-4} torr-sec at 1440 K. A boron oxide species from a lesser oxygen exposure ($7x10^{-5}$ torr-sec) and lower temperature (1270 K) is shown for comparison. Curve a: La; curve b: LaO; curve c: BO. The vertical amplification factor for each curve is shown and is relative to other desorption spectra.

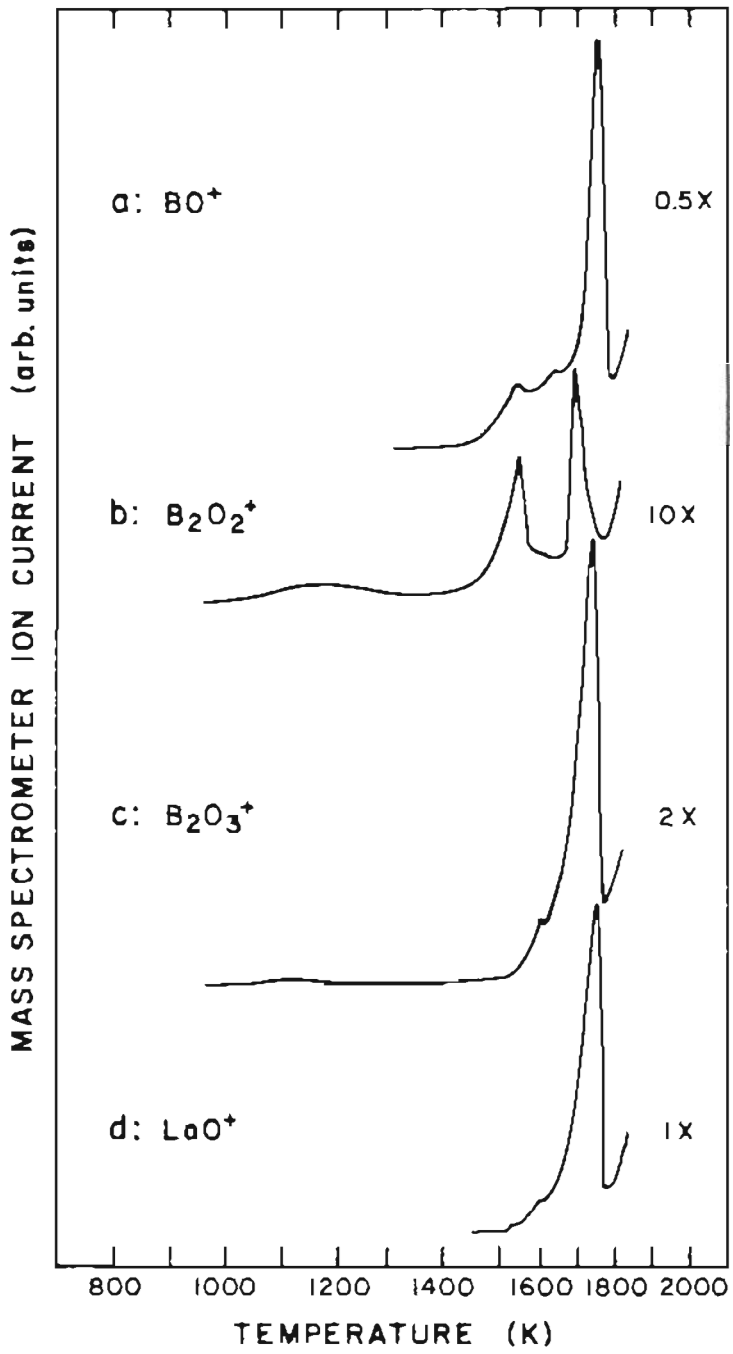

Figure 12 Thermal desorption of oxide species from LaB_6(310) after an oxygen exposure of 1.2×10^{-3} torr-sec at 1600 K. Curve a: BO; curve b: B_2O_2; curve c: B_2O_3; curve d: LaO. the vertical amplification factor for each curve is shown and is relative to other desorption spectra.

to occur around 1150 K but the amount actually desorbed at this temperature is very small compared to that at higher temperatures. A roughly equivalent amount of B_2O_3 is desorbed at this temperature, but again all parts of the curve occurring at higher temperatures can be attributed to the detection of doubly ionized La. Sharp peaks occurring at 1550 K are evident in the BO and B_2O_2 spectra, followed by a small peak at 1620 K which is seen in all the desorption curves. Finally, another large sharp peak in all of the desorption curves in observed at 1700 K. It is at this temperature where most desorption seems to occur.

Figure 13 shows the AES surface profile for a similarly oxidized surface. Changes in the surface become apparent at 1000 K where a rise in the boron signal and a fall in the oxygen signal occur. Surface conditions are relatively stable from 1100 K through 1300 K, where the boron signal rises to its maximum and oxygen begins to leave the-surface. It is not until 1750 K that the surface becomes oxygen free. The lanthanum signal is again quite stable, showing a small peak at 1400 K and slow decline at higher temperatures.

Observations were then made with the sample exposed to continuous oxygen pressures during heating cycles. Figures 14 and 15 show AES surface profiles of the surface under an oxygen pressure of $2x10^{-7}$ Torr with increasing and decreasing temperature, respectively. Surface compositions at room temperature for the two cases are not equivalent, the upsweep profile showing monolayer oxygen coverage while the downsweep profile indicates a much heavier oxide layer. A superficial examination of each elemental spectrum indicates that the reactions

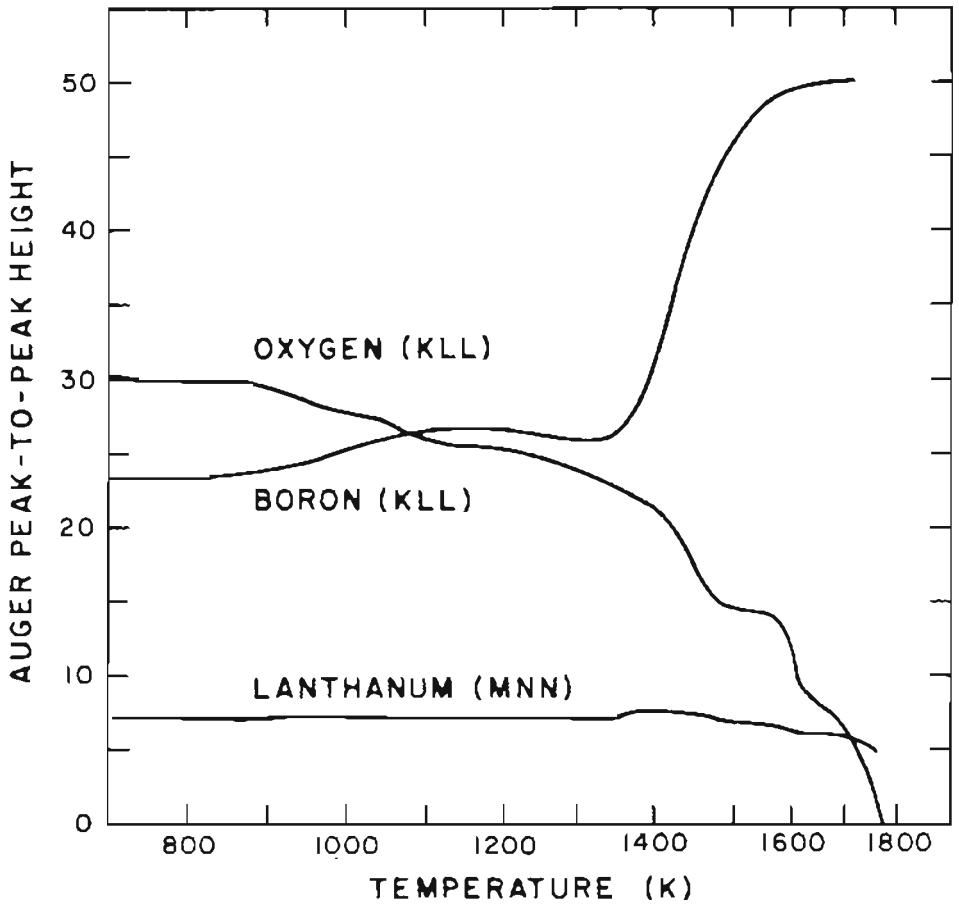

Figure 13 Variation with increasing temperature of boron, oxygen, and lanthanum Auger peak-to-peak heights of LaB_6 after an oxygen exposure of $2x10^{-3}$ torr-sec at 1600 K.

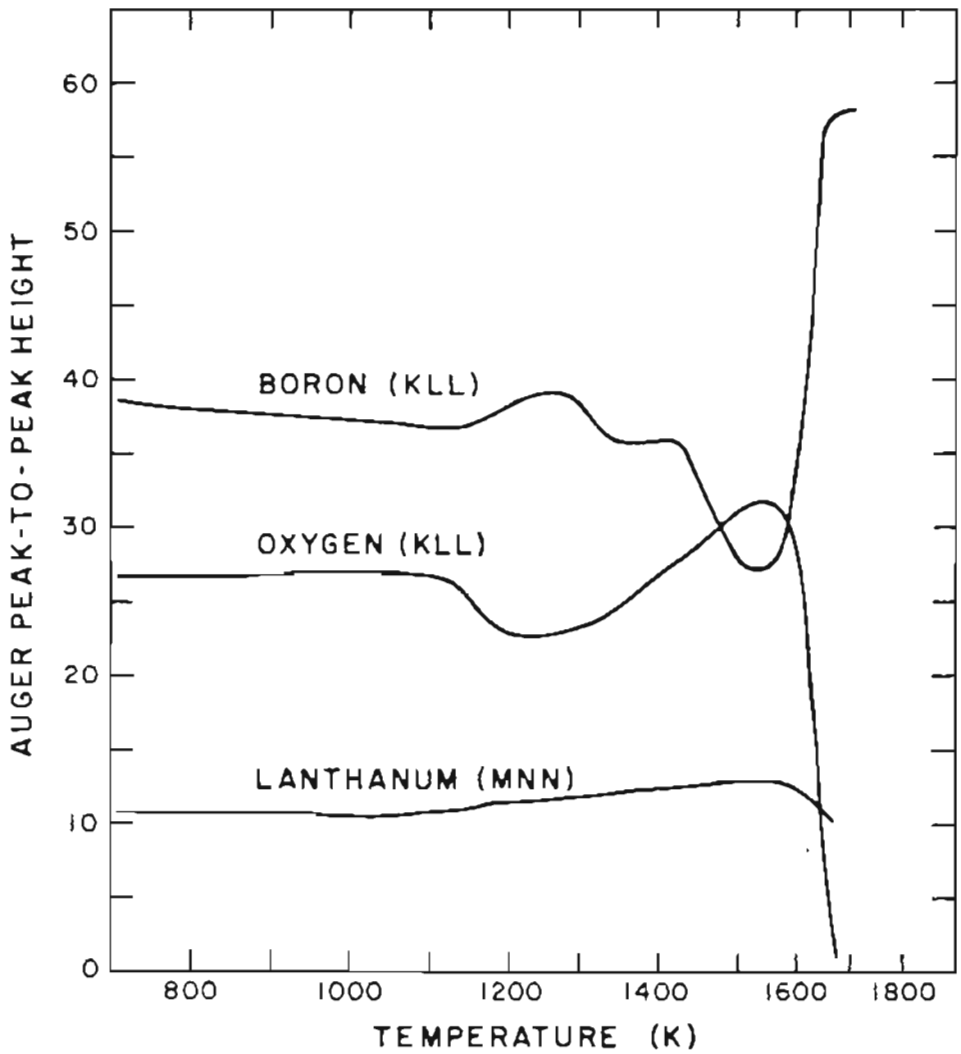

Figure 14 Variation with increasing temperature of boron, oxygen, and lanthanum Auger peak-to-peak heights of LaB_6(310) in an oxygen pressure of $2x10^{-7}$ torr.

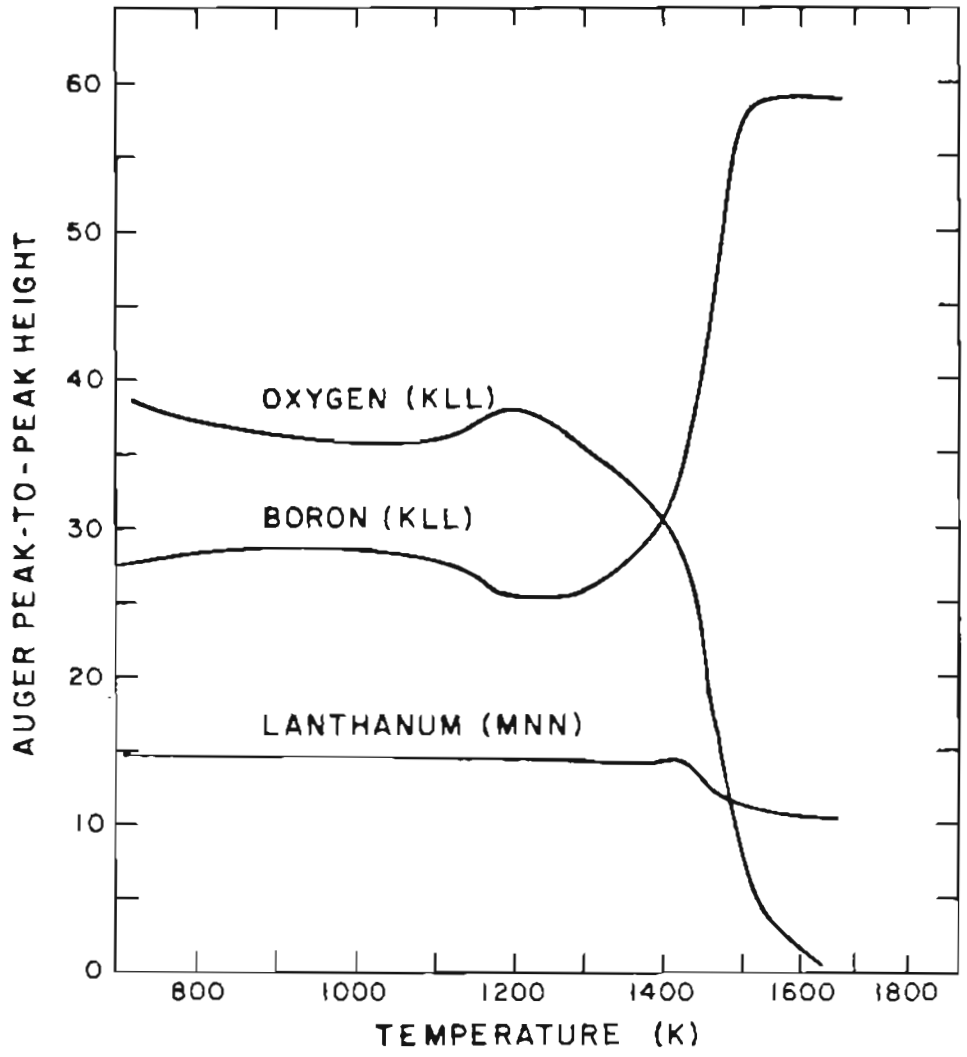

Figure 15 Variation with decreasing temperature of boron, oxygen, and lanthanum Auger peak-to-peak heights of LaB_6(310) in an oxygen pressure of $2x10^{-7}$ torr.

that are occurring on the surface are irreversible. The boron signal in the upsweep profile has several oscillations after 1100 K which suggest some type of boron oxide desorption. The boron signal from the decreasing temperature profile has only one broad minimum at 1250 K before stabilizing.

Thermal desorption spectra shown in Figure 16 also illustrate the irreversibility of the reactions. Boron and lanthanum desorption spectra were chosen in this case because, due to fragmentation, there is an echoing of other desorption products in the curves. The arrows on each curve denote the direction of temperature sweep, and due to the size of the sample there is roughly a 100 degree shift in measured temperature between upsweep and downsweep curves at 1100 K which reduces to zero around 1700 K. Apparent nonlinearities in the temperature of the downsweep curves are caused by inconsistencies in instrumentation. As can be seen the upsweep curve of the B desorption spectrum exhibits several sharp peaks whereas on decreasing temperature there are only two broad peaks. The La desorption spectrum shows similar features, a sharply peaked structure with increasing temperature and a smoothly descending curve with decreasing temperature.

All other desorbing species monitored are shown in Figure 17 with boron and lanthanum yields from the clean surface included for comparison. Clearly the added oxygen has increased the volatility of the surface, and LaO appears as the dominant desorption product from the surface at higher temperatures while B_2O_2 is dominant at lower temperatures.

Interaction of oxygen with the surface produced facetting of

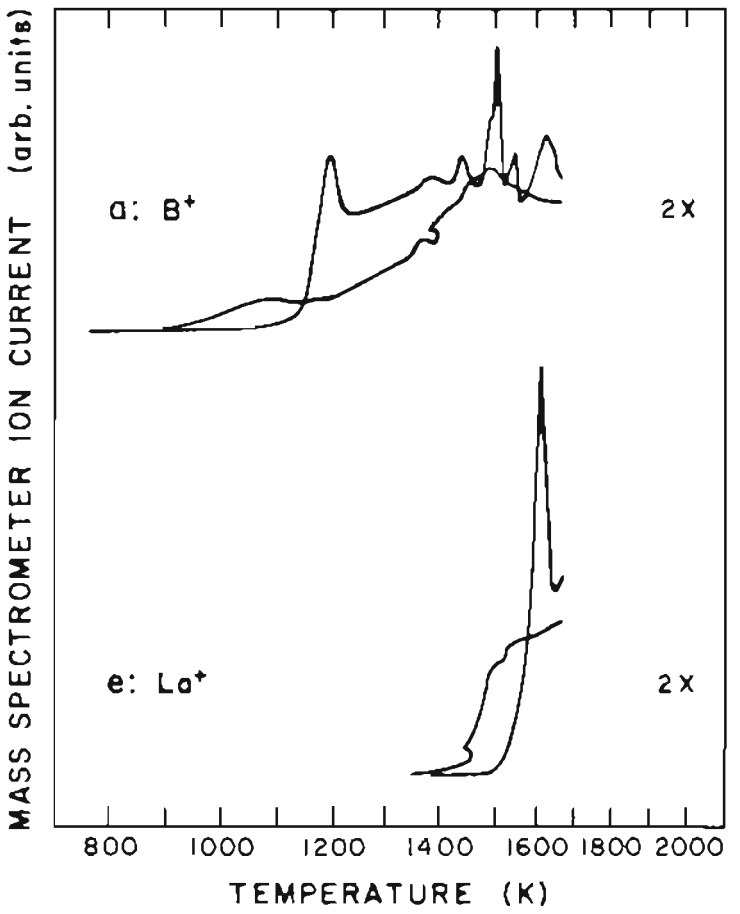

Figure 16 Relative desorption yields for B and La from LaB_6(310) as a function of temperature in an oxygen pressure of $2x10^{-7}$ torr. Arrows denote direction of temperature sweep.

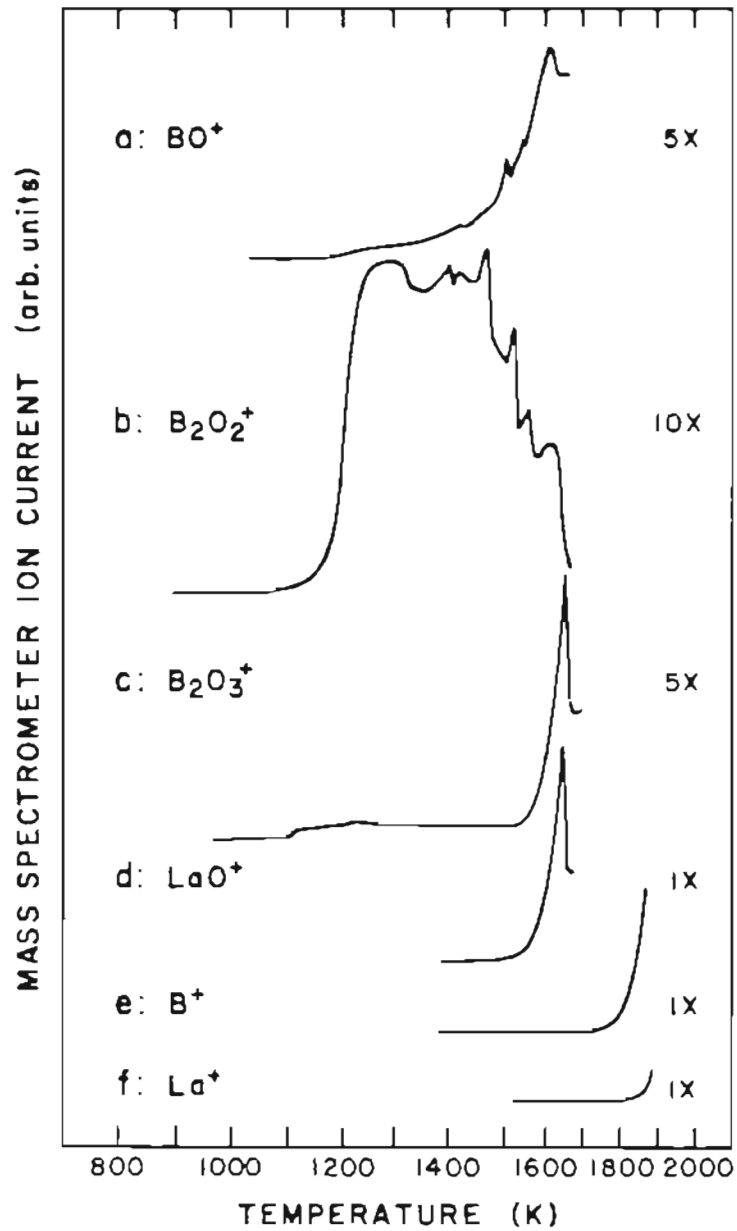

Figure 17 Relative desorption yields of BO, B_2O_2, B_2O_3, and LaO from LaB_6(310) as a function of increasing temperature in an oxygen pressure of $2x10^{-7}$ torr. Yields of B and La (curves e and f) from the clean surface are included for comparison.

the surface, as seen in Figure 18. The sample itself is pictured in Figure 18a and the view shown in 18b is from a location on the surface containing a defect in the crystal, in this case a rectangular hole in the surface. Angular measurements between this hole and the initial (310) surface give a divergence of 18 ± 3 degrees, a value in good agreement with that for [100] planes. The fact that the observed facets share angular directions with this hole provides evidence that they are also [100] planes. Work function measurements on the facetted surface give a value of 2.65 ± 0.5 eV, also consistent with the [100] surface of LaB_6. Other investigators have observed similar facetting of the (100), (110), and (111) surfaces of LaB_6 [10].

a:

b:

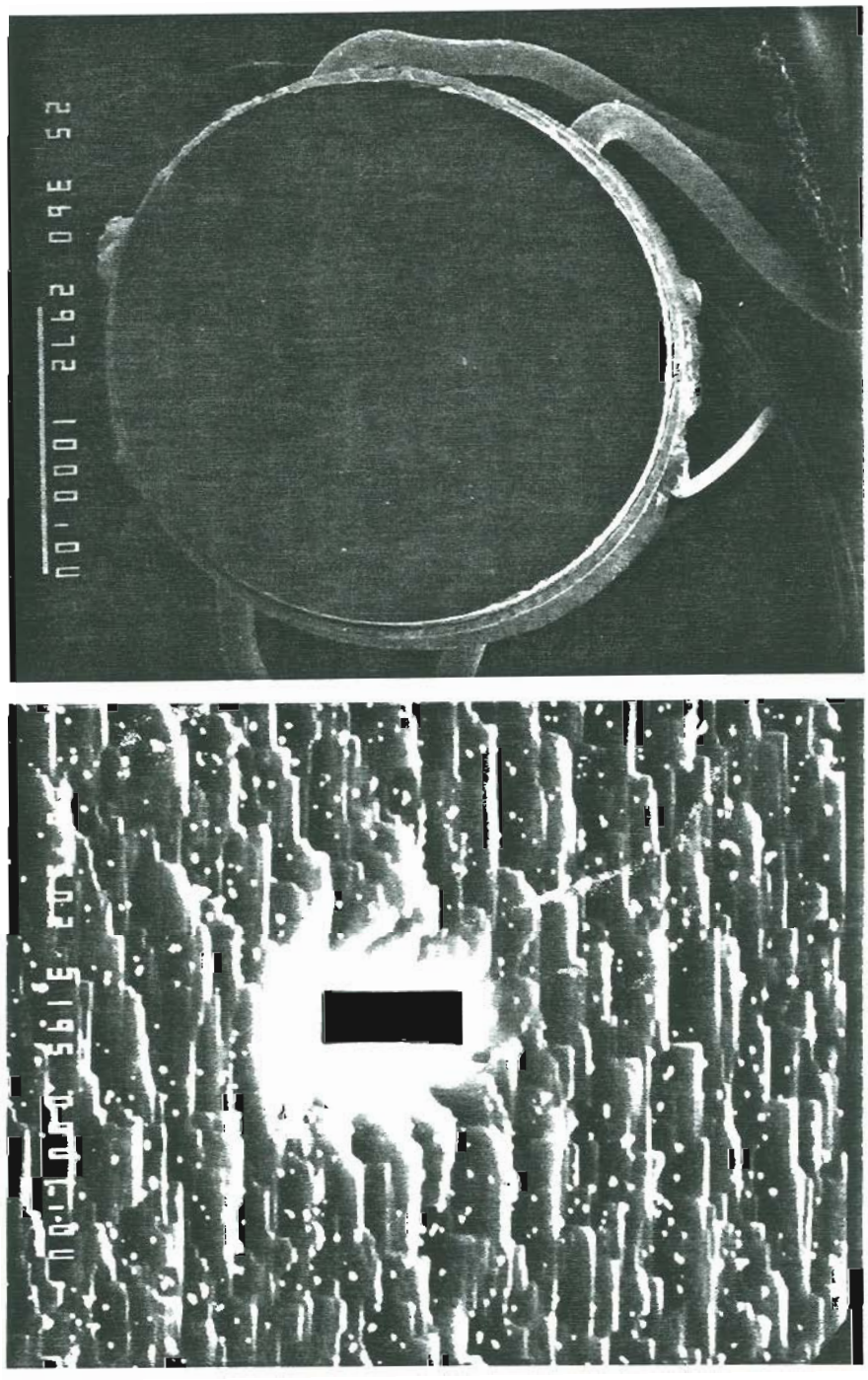

Figure 18 Electron micrographs of the LaB_6(310) sample used in the experiments. Photograph a: the sample magnified 50x; photograph b: a portion of the sample magnified 10kx showing facets and a crystal defect in the <100> direction.

IV. DISCUSSION

The interaction of oxygen with the (310) surface of LaB_6 has been investigated using Auger electron spectroscopy and mass spectroscopic analysis. Oxygen was either adsorbed on the surface in finite amounts or was continually present at pressures defined by experimental procedures. It was found that oxygen buildup on the surface saturates rapidly at room temperature and $P < 10^{-6}$ torr, or can form a thicker oxide layer at higher temperatures of adsorption.

The oxygen exposure necessary to effect saturation at room temperature was found to be 50L. This exposure is more than three times as much as that reported for the (110) surface (<16L) [15,18],the (100) or (111) surfaces (<15L) [12], or the (210) surface (15L) [16]. The implication is that the sticking coefficient of oxygen on the (310) surface is considerably less than on the other surfaces studied, although this aspect has not been studied in detail.

Changes in the Auger spectra of Figure 5 are due to chemical bonding on the surface. As outlined in ref. [8] the portion of the boron peak between 175 and 200 eV separates into two peaks, the lower eV peak corresponding to oxide-state B while the higher eV peak corresponds to elemental B. The portion of the lanthanum peak between 620 and 650 eV can be treated similarly, with more splitting corresponding to an increase of oxide-state La in the surface layer. The boron spectrum of curve c) in Figure 5 would then indicate more elemental B than oxide state B and curve b) would show virtually all

oxide state B. Similarly, the lanthanum spectrum in curve c) shows far more oxide state La than its counterpart in curve b). These findings are corroborated by desorption spectra produced from the same oxidizing conditions, Figures 7 and 8 and Figures 10 and 11 corresponding to curves 5b and 5c, respectively. The proportion of boron oxides relative to lanthanum oxides observed after lower temperature oxidation is greater than the proportion observed after higher temperature oxidation.

Chemical composition of the oxide formed on the surface is also of interest, and while the exact composition cannot be determined using the methods presented here, certain comparisons can be made. The boron spectrum shown in Figure 5c compares favorably with the spectrum observed from B_2O_3 by Hanke and Muller [20]. There is some disparity in the lower portion of the boron spectrum, notably the relative heights of the elemental and oxide state peaks, but overall the curve shapes are quite similar. Experiments on $LaB_6(100)$ performed by Futamoto et al. [11] under similar oxidizing conditions found evidence of La_2O_3 on the surface. It is not unreasonable to assume that the lanthanum oxide seen on $LaB_6(310)$ is also La_2O_3. Therefore the oxide layer seen on $LaB_6(310)$ is probably a combination of B_2O_3 and La_2O_3, the exact proportion of each oxide dependent on oxidizing conditions.

More information on the composition of this oxide layer can be found in the AES surface profiles obtained while heating in constant pressures of oxygen as in Figures 14 and 15. Exact proportions of elements in the oxide cannot be found since the profiles observed while raising sample temperature also contain desorption information, and

those obtained when lowering sample temperature are complicated by the formation of oxide layers on top of those layers already formed. It is clear, however, that oxides of different compositions are being formed at different temperatures, a more boron rich oxide at lower temperatures and a lanthanum rich oxide at higher temperatures.

Thermal desorption studies provide information about the nature of surface oxide species and, when combined with Auger measurements on preadsorbed layers of oxygen, about relative positions of oxygen binding sites on the surface. Before proceeding further, however, there are several points which must be considered in order to view the data from the proper perspective.

The first point is the apparent stability of the lanthanum Auger peak to peak height as shown in Figures 6, 9, and 13. At first glance it would appear that the lanthanum content of the surface layer is unchanging and only boron and oxygen content vary to any degree. This apparent stability is influenced by three factors and should therefore be treated accordingly. First, as described by Spicer and Landau [21], the Auger electron escape depth from any surface is to first order dependent on electron energy, with small escape depths for lower energy electrons and larger escape depths for higher energy electrons. Apparent lanthanum surface concentrations (625 eV Auger electrons) are therefore more indicative of unchanging bulk composition than are the measured boron (179 eV) or oxygen (503 eV) surface concentrations. Second, as can readily be seen in Figure 5 the lanthanum peak shape is visibly influenced by chemical bonding. Thus, the peak-to-peak height in the derivative mode is not a precise measure of the surface La

concentration. Finally, it was found by Aono et al. [9] that surface La atoms on LaB_6(100) exhibit vigorous thermal motion at 1400 K or above. Since this motion precedes any desorption of LaO from the surface additional effects on the La Auger peak shape are possible.

The next point is that fragmentation of desorption products occurs within the mass analyzer ionization section. Examination of the desorption product curves of Figures 7 and 8 suggests that B_2O_2 is being broken down into BO, B, and O and that LaO is converted to La and O. In addition to difficulties in assigning relative yields of desorption products, this fragmentation could conceal desorption of elemental B and La from the surface. A detailed examination of this problem, not undertaken in this project, would be necessary to resolve these questions.

Despite these difficulties there is still much information that can be obtained from the desorption product spectra and AES surface profiles. Using the Redhead technique [22] it is possible to assign binding energies to the observed desorption products. The binding energies found in this study for LaB_6(310) are compared to those found for LaB_6(100) [13] and LaB_6(110) [15], and are shown in Table 2. The deviations of the binding energies for BO and LaO among the different surfaces can probably be attributed to different amounts of oxygen adsorbed on each surface before desorption. If more oxygen is adsorbed on LaB_6(310) the desorption peaks begin at the same temperature but reach their respective maxima at higher temperatures, since it is at this point that all oxygen is removed from the surface.

It is also interesting to note that as the adsorption temperature

	BINDING ENERGY (eV)[a]		
Species	$LaB_6(310)$[b]	$LaB_6(100)$[c]	$LaB_6(110)$[d]
BO	4.7 + 0.2	3.6 ± 0.1 4.3 ± 0.1	3.4 3.9 4.1
B_2O_2	3.7 ± 0.1	3.3 ± 0.1 3.5 ± 0.1	—
B_2O_3	3.4 ± 0.1	3.4 ± 0.1	—
LaO	4.6 ± 0.1	4.3 ± 0.2	4.2

[a] determined by the Redhead method

[b] after oxygen adsorption at 300 K

[c] from reference [13]; after oxygen adsorption at 1000 K

[d] from reference [15]; after oxygen adsorption at 300 K

Table 2 Thermal desorption of oxides from LaB_6: Binding energies.

increases so do the binding energies of the desorption products, which slowly approach the same value of 4.9±0.1 eV as adsorption temperature is increased. The higher adsorption temperature apparently prevents the formation of lower energy bound states while creating a thicker oxide coating that contains fewer surface oxide states.

Among all monitored desorption products BO can be considered to be the dominant boron oxide desorbed, even if all the observed elemental B is considered to originate from B_2O_2. The major boron oxide desorption product from $LaB_6(100)$ was found to be B_2O_2 [13], implying that surface structure plays some role in the formation of these oxides. Since all oxygen is removed from the surface at temperatures above 1500 K it is evident that BO and LaO are the dominant desorption products here.

Using Auger electron spectroscopy in conjunction with mass spectrometric analysis for oxide evaporation studies allows a more precise determination of the relative amount of desorbing species than would be possible using either method separately. The desorption of boron oxides is visible in the AES surface profiles as abrupt increases in the boron signal and simultaneous decreases in the oxygen signal. These changes are seen primarily because of an increase of boron and decrease of oxygen in the surface layer probed by AES as oxides are desorbed, but are also due to AES peak shape changes as the desorption occurs. However, it is true that most oxygen adsorbed on the surface at room temperature is removed at temperatures above 1400 K. Thus, since BO and LaO are the only desorption products observed above this temperature it follows that they are the dominant desorption products,

in agreement with the mass spectrometric desorption data. Unfortunately, the narrow range of desorption temperatures for oxidation at higher temperatures precludes a similar analysis. Nevertheless, the confirmation of the desorption product amounts following room temperature oxidation supports the results of mass spectrometric analysis.

It could be possible to describe the major desorption reactions by the equations

$$O_2(g)=2O(a) \tag{1}$$

$$B+O(a)=BO(a), \quad k_1 \tag{2}$$

$$BO(a)=BO(g), \quad k_2 \tag{3}$$

$$2BO(a)=B_2O_2(g), \quad k_3 \tag{4}$$

$$La+O(a)=LaO(a), \quad k_4 \tag{5}$$

$$LaO(a)=LaO(g), \quad k_5, \tag{6}$$

where the (g) and (a) correspond to gas and adsorbed phase, respectively, and the k associated with each reaction corresponding to its rate constant. Then under steady state conditions the coverage of O, BO, B_2O_2, and LaO are unchanging so their derivatives may be written as

$$\frac{d\sigma_1}{dt} = \frac{Ps}{(2\pi mkT)^{1/2}} - (k_2+k_5)\sigma_1 = 0 \tag{7}$$

$$\frac{d\sigma_2}{dt} = k_1\sigma_1 - k_2\sigma_2 - k_3\sigma_2^2 = 0 \tag{8}$$

$$\frac{d\sigma_3}{dt} = k_4\sigma_1 - k_5\sigma_3 = 0 \tag{9}$$

where σ_1, σ_2, and σ_3 are coverages of O, BO, and LaO, respectively, P is the oxygen pressure, k is Boltzman's constant, and s is the sticking coefficient which is a function of temperature. Solving these equations for the coverages results in

$$\sigma_1 = \frac{Ps}{(k_2+k_5)(2\pi mkT)^{1/2}} \tag{10}$$

$$\sigma_2 = \frac{-k_2+[k_2^2+4k_1k_3Ps/(k_2+k_5)(2\pi mkT)^{1/2}]^{1/2}}{2k_3} \tag{11}$$

$$\sigma_3 = \frac{k_4Ps}{k_5(k_2+k_5)(2\pi mkT)^{1/2}} \tag{12}$$

The rate of evolutions of the gaseous phases of BO, B_2O_2, and LaO are then

$$R(BO) = \frac{k_2(-k_2+[k_2^2+4k_1k_3Ps/(k_2+k_5)(2\pi mkT)^{1/2}]^{1/2})}{2k_3} \tag{13}$$

$$R(B_2O_2) = \frac{k_3(-k_2+[k_2^2+4k_1k_3Ps/(k_2+k_5)(2\pi mkT)^{1/2}]^{1/2})^2}{4k_3^2} \tag{14}$$

$$R(LaO) = \frac{k_5k_4Ps}{k_5(k_2+k_5)(2\pi mkT)^{1/2}} \tag{15}$$

From these equations it is possible to make the following predictions about the steady state evolution of the main desorption pro-

ducts: 1) the pressure dependence of the LaO desorption spectrum is linear, while the pressure dependence of the BO and B_2O_2 desorption spectra is a quadratic function; 2) a maximum in the Lao desorption spectrum can occur only if the sticking coefficient goes to zero at high temperatures; 3) maxima in the desorption spectra of BO and B_2O_2 are possible either from a decrease in the sticking coefficient at high temperatures or from the change of the rate constants with temperature. Further investigations are necessary verify these predictions.

V. CONCLUSION

The rate of oxygen adsorption on LaB_6(310) was found to be much slower than on any other surface of LaB_6 studied. Oxides formed on the surface after oxygen adsorption at higher temperatures consist of a mixture of boron oxide, B_2O_3, and lanthanum containing oxide, possibly La_2O_3, where the proportion of each oxide formed depends on oxidizing conditions, notably oxygen pressure and surface temperature. The composition of the lanthanum containing oxide has not been conclusively established. Most oxygen is desorbed from the surface in the form of BO at temperatures below 1500 K and in the form of LaO above 1500 K. Other boron oxides are desorbed below 1500 K but do not contribute greatly to the total amount of oxide removed. The surface can therefore become more or less lanthanum rich, depending on the desorption temperature. In constant pressures of oxygen the surface is modified predominantly by the removal of B_2O_2 at temperatures below 1400 K, by the removal of BO between 1400 and 1500 K, and by the removal of LaO at temperatures above 1600 K. Exposure of the surface to oxygen at steady pressures below 10^{-6} torr and temperatures higher than 1700 K does not cause detectable oxygen adsorption nor desorption of oxygen-containing species. Oxygen interaction with the surface at intermediate temperatures induces facetting of the (310) surface into (100) planes, the resultant surface showing a work function of 2.65 ± 0.5 eV. Implications of this result from the point of view of cathode applications are, 1) after a significant exposure to oxygen at elevated temperatures

operating temperatures must be increased for comparable emission, or, 2) in order to maintain the (310) surface structure and its emission characteristics, operation of the cathode must be under oxygen pressures of less than 10^{-9} torr for temperatures less than 1700 K.

REFERENCES

1. J.M. Lafferty, J. Appl. Phys. 22 (1951), 229.

2. L.W. Swanson, M.A. Gesley, and P.R. Davis, Surface Sci. 107 (1981), 263.

3. C. Oshima, M. Aono, T. Tanaka, S. Kawai, R. Shimizu, and H. Hagiwara, J. Appl. Phys. 51 (1980), 1201.

4. R. Nishitani, M. Aono, T. Tanaka, C. Oshima, S. Kawai, H. Iwasaki, and S. Nakamura, Surface Sci. 93 (1980), 535.

5. C. Oshima, M. Aono, T. Tanaka, and S. Kawai, J. Appl. Phys 51 (1980), 997.

6. M. Gesley and L.W. Swanson, Surface Sci. 146 (1984), 583.

7. M. Aono, T. Tanaka, E. Bannai, and S. Kawai, Appl. Phys. Letters 31 (1977), 323.

8. B. Goldstein and D.J. Szostak, Surface Sci. 74 (1978), 461.

9. M. Aono, R. Nishitani, C. Oshima, T. Tanaka, E. Bannai, and S. Kawai, J. Appl. Phys. 50 (1979), 4802.

10. S.J. Klauser and E.B. Bas, Appl. Surf. Sci.3 (1979), 356.

11. M. Futamoto, M. Nakazawa, K. Usami, S. Hosoki, and U. Kawabe, J. Appl. Phys. 51 (1980), 3869.

12. R. Nishitani, S. Kawai, H. Iwasaki, S. Nakamura, M. Aono, and T. Tanaka, Surface Sci. 92 (1980), 191.

13. P.R. Davis and S.A. Chambers, Appl. Surf. Sci. 8 (1981), 197.

14. R. Nishitani, C. Oshima, M. Aono, T. Tanaka, S. Kawai, H. Iwasaki, and S. Nakamura, Surface Sci. 115 (1982), 48.

15. E.B. Bas, P. Hafner, and S. Klauser, in: Proc. 7th Intern. Vacuum Congr. and 3rd Intern. Conf. Solid Surfaces (Vienna, 1972), 881.

16. C. Oshima, T. Tanaka, R. Nishitani, and S. Kawai, J. Appl. Phys. 51 (1980), 997.

17. M.A. Noack, M.Sc. Thesis, Iowa State University, Ames, Iowa (1979).

18. E.K. Storms, J. Appl. Phys. 50 (1979), 4450.

19. T.E. Madey and J.T. Yates, J. Vac. Sci. Tech. 8 (1971), 525.

20. G. Hanke and K. Muller, J. Vac. Sci. Technol. A2(2) (1984), 964.

21. I. Landau and W.E. Spicer, J. Electron Spectrosc. Related Phenomena 3 (1974), 461.

22. P.A. Redhead, Vacuum 12 (1962), 1203.

BIOGRAPHICAL NOTE

The author was born 15 December 1960, in Arvada, Colorado. He continued his residence in that city, attending public schools until his graduation from Arvada Senior High School in 1979. He then entered Colorado State University where he received his Bachelor of Science degree with honors in May, 1983.

In September of that same year he began study at the Oregon Graduate Center where he completed the requirements for the degree Master of Science in September, 1985.

He is leaving the Graduate Center to live in the state of Colorado.